PLOS ONE

RESEARCH ARTICLE

CD147 mediates intrahepatic leukocyte aggregation and determines the extent of liver injury

Christine Yee[1,2☯], Nathan M. Main[2☯], Alexandra Terry[1,2☯], Igor Stevanovski[2], Annette Maczurek[1], Alison J. Morgan[1], Sarah Calabro[1], Alison J. Potter[1], Tina L. Iemma[1], David G. Bowen[1,3], Golo Ahlenstiel[4], Fiona J. Warner[1], Geoffrey W. McCaughan[1,3], Susan V. McLennan[5], Nicholas A. Shackel[1,2,3,6]*

1 Centenary Institute of Cancer Medicine and Cell Biology, The University of Sydney, NSW, Australia, **2** Gastroenterology and Liver Laboratory, Ingham Institute for Applied Medical Research, Liverpool, NSW, Australia, **3** A.W. Morrow Gastroenterology and Liver Centre, Royal Prince Alfred Hospital, Camperdown, NSW, Australia, **4** Western Sydney School of Medicine, Blacktown Hospital, Blacktown, NSW, Australia, **5** Department of Endocrinology, Department of Medicine and Bosch Institute, Royal Prince Alfred Hospital, The University of Sydney, NSW, Australia, **6** Liverpool Hospital, Liverpool, NSW, Australia

☯ These authors contributed equally to this work.
* n.shackel@unsw.edu.au

Citation: Yee C, Main NM, Terry A, Stevanovski I, Maczurek A, Morgan AJ, et al. (2019) CD147 mediates intrahepatic leukocyte aggregation and determines the extent of liver injury. PLoS ONE 14 (7): e0215557. https://doi.org/10.1371/journal.pone.0215557

Editor: Partha Mukhopadhyay, National Institutes of Health, UNITED STATES

Received: April 2, 2019

Accepted: June 24, 2019

Published: July 10, 2019

Data Availability Statement: All relevant data are within the manuscript and its Supporting Information files.

Funding: This work was funded by the NMHRC, Project Grant IDs: 1063515, 512283. The funder had no role in study design, data collection and analysis, decision to publish, or preparation of the manuscript.

Competing interests: The authors have declared that no competing interests exist.

Abstract

Background

Chronic inflammation is the driver of liver injury and results in progressive fibrosis and eventual cirrhosis with consequences including both liver failure and liver cancer. We have previously described increased expression of the highly multifunctional glycoprotein CD147 in liver injury. This work describes a novel role of CD147 in liver inflammation and the importance of leukocyte aggregates in determining the extent of liver injury.

Methods

Non-diseased, progressive injury, and cirrhotic liver from humans and mice were examined using a mAb targeting CD147. Inflammatory cell subsets were assessed by multiparameter flow cytometry.

Results

In liver injury, we observe abundant, intrahepatic leukocyte clusters defined as $\geq$5 adjacent $CD45^+$ cells which we have termed "leukocyte aggregates". We have shown that these leukocyte aggregates have a significant effect in determining the extent of liver injury. If CD147 is blocked *in vivo*, these leukocyte aggregates diminish in size and number, together with a marked significant reduction in liver injury including fibrosis. This is accompanied by no change in overall intrahepatic leukocyte numbers. Further, blocking of aggregation formation occurs prior to an appreciable increase in inflammatory markers or fibrosis. Additionally, there were no observed, "off-target" or unpredicted effects in targeting CD147.

Conclusion

CD147 mediates leukocyte aggregation which is associated with the development of liver injury. This is not a secondary effect, but a cause of injury as aggregate formation proceeds other markers of injury. Leukocyte aggregation has been previously described in inflammation dating back over many decades. Here we demonstrate that leukocyte aggregates determine the extent of liver injury.

Introduction

The classical hallmark of liver injury is the deposition of abnormal/fibrotic extracellular matrix (ECM) and the eventual development of cirrhosis, which is mediated by the activated hepatic stellate cell (HSC). Chronic inflammation drives ongoing HSC activation and fibrosis [1]. Chronic liver inflammation can be regarded as commencing with an initial innate immune response and progressing with an ongoing insult, into a chronic injury with both sustained innate and adaptive immune components [2–6]. T-cell responses are clearly pivotal to the development of chronic immune-mediated hepatic injury and it has now been shown that B-cells are essential for the development of intrahepatic fibrosis leading to cirrhosis [7–11].

Importantly, we have previously identified a number of novel pathways of liver injury [12–14]. Arising from these studies, we have shown that hepatocytes remodel extracellular matrix in liver injury via the production of active matrix-metalloproteinases [15].

CD147 is an abundant 269aa type 1 integral glycosylated and multifunctional membrane protein with different cellular functions on differing cell sub-populations. The concept of multifunctional proteins is well established [16–20], with at least 3% of all proteins in the human protein interaction network being classified as 'extreme multifunctional' proteins [20]. CD147 is expressed within a wide range of tissues, including endothelium and epithelium [21–23]. CD147 is thought to act via MAPK p38, ERK-1, -2, PI3K and NF-KB signalling pathways [24–27]. The regulation of CD147 expression is largely uncharacterised.

A striking and consistent function attributed to CD147 is its ability to regulate leukocyte chemotaxis. Cyclophilins (CyP)-A and B are two CD147 ligands known to mediate chemotaxis [21,28–30]. CD147 has been shown to be important for leukocyte recruitment in rheumatoid arthritis, multiple sclerosis and inflammatory lung disease, with mAb αCD147 interventions leading to reduced neutrophil, T-cell and monocytes/macrophage infiltration [11,28,31–37].

CD147 is mostly found in membrane protein complexes [29,30,38–40] and many of its binding partners are matrix components or inflammatory mediators that are dramatically increased with injury (i.e. hyaluronan [41], intercellular adhesion molecule (ICAM)-1 [38,42,43], lymphocyte function-associated antigen (LFA)-1 [44–46] and CD43 [47, 48]). Additionally, CD147 is also found in large complicated multiple protein "super-complexes" on the cell surface containing many binding partners [39]. Studies have shown that the domain of CD147 that mediates cell migration is distinct from the domain mediating MMP induction (within extracellular loop I) [49,50]. Therefore, it is well established that CD147 is a multifunctional protein [16–20] with distinct binding partners and structural domains determining its varied functions at specific cellular locations.

Leukocyte aggregations of either lymphoid or myeloid origin are thought to exacerbate inflammation and in turn, the severity of disease. In acute viral infection, TLR stimulation and TNF signalling induced myeloid cell aggregation in the liver [51]. These myeloid aggregates induced localized CD8+ T cell proliferation. Myeloid cell aggregation was not observed in

chronic viral infection. It is yet to be determined if immune cell aggregation occurs in non-viral induced liver injury. The molecules associated with immune aggregation are also unknown. Aggregation of leukocytes within the liver tissue during disease has been most observed in *H*epatitis *C V*irus (HCV) infection and *a*lcoholic *l*iver *d*isease (ALD), though their role in pathogenesis and mode of development is still unclear [52]. We have previously shown that CD147 is increased in cirrhotic liver and expressed by hepatocytes (not HSC) during progressive liver injury [15]. Herein, we report CD147 upregulation on multiple immune cell subsets during liver injury. This manuscript is the first description of a novel CD147-mediated mechanism of immune cell aggregation in liver injury. Specifically, we have shown that CD147-mediated immune cell aggregation is independent of cell proliferation and anti-CD147 intervention reduces immune cell aggregation.

Materials and methods

Human ethics

Human tissue samples were obtained from Royal Prince Alfred Hospital, Sydney with approval of the Human Research Ethics Committee (Proposal: X10-0072). Human tissue used in this study was previously utilized for research [12, 15]. Informed written consent was obtained from all participants. The ethics committee waived the need for written consent for use of donor tissue. In Australia, the ethics of human research is governed by the National Statement on Ethical Conduct in Human Research (2007) issued by the National Health and Medical Research Council (NHMRC). Under these guidelines, all research involving humans requires ethical approval. Non-diseased donor (n = 4) and end-stage cirrhotic liver tissues (n = 15) were collected from patients attending Prince Alfred Hospital, Sydney during liver transplantation.

Mice

Eight-week old male, wild-type mice (BALB/c and C57Bl/6) (n = 5–8 per group) were sourced from Animal Resources Centre (Canning Vale, WA, Australia) and housed at the Centenary Institute Animal facility (Camperdown, NSW, Australia) in compliance with the Animal Care and Ethics Committee at the University of Sydney (Prospectively approved protocol:K75/10-2008/3/4801). Liver injury was induced by either thioacetamide (TAA) (300mg/L) (MP Biomedicals, Ohio, USA) in drinking water *ad libitum* for four, eight or twenty weeks, or by carbon tetrachloride (CCl_4) (Univar, Ajax Chemicals, Sydney) via intraperitoneal injection (i.p) with 100μl of 12% CCl_4 in paraffin oil mixture once (one day) or twice weekly for four weeks. Control mice were injected with paraffin oil alone (PO). Both treated and age-matched control mice were sacrificed by CO_2 asphyxiation at conclusion of treatment. CD147 antibody was administered by i.p injection twice weekly (100μg) and control mice received IgG2a (100μg) (HB-189, ATCC). The rat anti-mouse IgG2a CD147 blocking antibody (mAb RL73.2) was produced by hybridoma cells and purified as described [53].

Primary cell isolation

Primary hepatocytes and leukocytes were isolated using a 2-step collagenase-perfusion technique based on Howard et al.[54]. Briefly, livers were perfused *in situ* with collagenase IV (Sigma-Aldrich, St. Louis, USA) and removed for density gradient centrifugation with isotonic Percoll (GE Healthcare Life Sciences, Chicago, USA) for separation of the hepatocytes (pellet) and leukocytes (supernatant) from a mixed population. The two phases were further separated, washed and resuspended to form a single cell suspension for flow cytometry, or centrifuged and pelleted for snap frozen storage at -80˚C prior to downstream RNA or protein isolation.

For peripheral blood mononuclear cell (PBMC) isolation, peripheral blood from the inferior vena cava was collected into 500μl of ice-cold Alsever's solution (Sigma-Aldrich) prior to erythrocyte removal, washing and resuspension to form a single cell suspension for flow cytometric analyses. Further aliquots were pelleted by centrifugation for snap frozen storage at -80˚C prior to downstream RNA extraction. Similarly, for splenocyte isolation, whole tissue was mechanically disrupted and passed through a 50μm sieve, prior to erythrocyte removal, washing and resuspension to form a single cell suspension for flow cytometric analyses.

Gene expression analysis

Total RNA from liver leukocytes, hepatocytes, and whole liver were isolated with TRIzol reagent (Invitrogen, San Diego, CA) and cDNA synthesized with SuperScript™ III Reverse Transcriptase (Invitrogen). Quantitative RT-PCR was performed using SYBR® green fluorescent dye (Invitrogen). Specific Taqman probes were used for amplification of CD147 (forward 5'-GTCCAGGAAGTCAACTCCAA-3'; reverse, 5'-GCTCAGGAAGGAAGATGCAG-3') and this was normalised to housekeeping control 18S (forward, 5′-CGGCTACCACATCCAAGGA-3′; reverse, 5′- CTGGAATTACCGCGGCTG-3).

Liver function tests

Blood was collected from the inferior vena cava into MiniCollect Serum Tubes (Greiner Bio-One, Kremsmünster, Germany). Serum was isolated by centrifugation at 3000 *r*elative *c*entrifugal *f*orce (RCF) for 10 minutes and the supernatant was collected. Serum was diluted 1:3 in PBS and tested for the activity of enzymes *al*kaline *p*hosphatase (ALP), *al*anine *t*ransaminase (ALT) and *as*partate *t*ransaminase (AST) by the Sydney South West Pathology Service. All results are measured in international units per litre (U/L).

Flow cytometry of CD147 surface expression on leukocyte subsets

Flow cytometry was performed on isolated liver and spleen leukocytes from control and TAA-treated mice. Cells were co-stained with antibodies against CD3ε - PE/Cy7 (145-2C11, BioLegend, San Diego, USA), CD4-Pacific orange (RM4-5, Invitrogen), CD8α –Pacific blue (53–6.7, BioLegend), CD19 –AlexaFlour 488 (6D5, BioLegend), NK1.1-PE (PK136, BD Biosciences, San Jose, USA), F4/80-PerCP/Cy5.5 (RM8, BioLegend) and CD147 –biotin (OX114, BioLegend) further stained with Streptavidin-APC (Invitrogen). Flow cytometry data were collected with FACS LSR-II (BD Biosciences). Each leukocyte subset was analysed for expression of CD147 and data recorded as median fluorescence intensity. Bar graphs represent mean ± SEM. Statistical analysis was performed by the Kruskal-Wallis test followed by Dunn's multiple comparisons test.

Immunofluorescence analysis

Indirect immunofluorescence was performed on frozen and fixed (acetone:methanol) liver tissue using monoclonal antibody CD45-FITC (1:100) (30-F11, BD Pharmingen, San Jose, USA). Co-localisation was assessed using CD147 (1:100) (RL73.2, hybridoma), Gr-1 (1:100) (RB6-8C5, BD Pharminogen) and F4/80 (1:200) (CI:A3-1, hybridoma), B220 (1:100) (RA3-6B2, BD Phaminogen), CD19 (1:100) (ID3, BD Pharmingen) and CD3e (1:100) (UCHT1, Dako). Secondary antibodies anti-rat AlexaFluor® 594 (1:200) (#A-11007, Molecular Probes) and goat anti-rabbit AlexaFluor® 633 (1:200) (#A-21071, Invitrogen) were used. For control of background staining, the primary antibodies were omitted or replaced by IgG isotype control (Cat

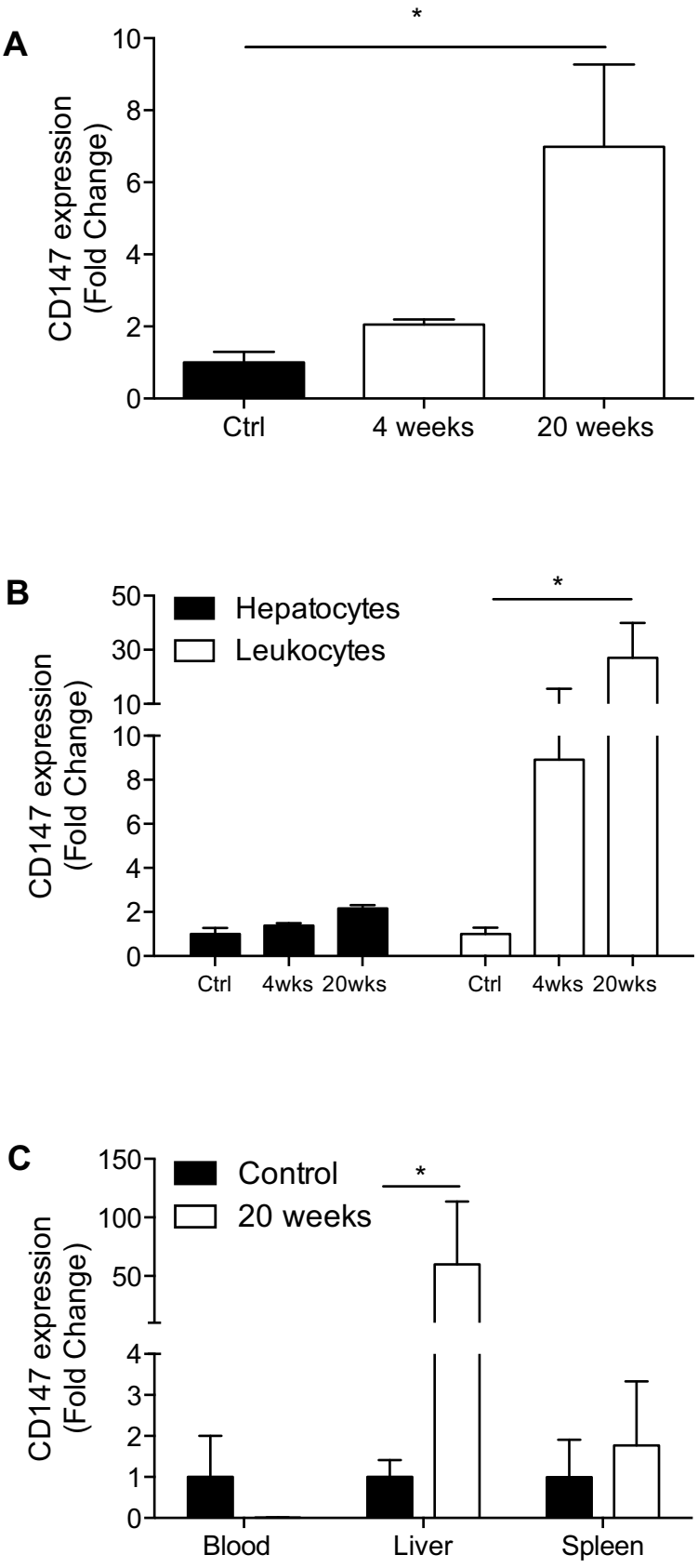
A
*
CD147 expression (Fold Change)
10
8
6
4
2
0
Ctrl
4 weeks
20 weeks
B
*
Hepatocytes
Leukocytes
CD147 expression (Fold Change)
50
30
10
10
8
6
4
2
0
Ctrl
4wks
20wks
Ctrl
4wks
20wks
C
Control
20 weeks
*
CD147 expression (Fold Change)
150
100
50
4
3
2
1
0
Blood
Liver
Spleen

Fig 1. Quantitative real-time PCR for CD147 expression in a mouse model of TAA-induced liver injury. (A) CD147 expression in whole liver from control, 4 week and 20-week TAA-treated mice. (B) Comparison of CD147 expression in liver leukocytes and hepatocytes throughout the course of TAA-induced injury. (C) CD147 expression in blood, liver, and spleen at 20 weeks compared to control. Data were normalised to 18S and expressed as fold change from control. Bars represent mean +SEM. Mann-Whitney test was performed to assess significance from control where * $p<0.05$ (n = 5–7 per group).

https://doi.org/10.1371/journal.pone.0215557.g001

ID: 559073, Dako, San Clara, USA). The fluorescent images were imaged using a Leica TCS SP5 II confocal microscope (Leica, Georgia, USA).

Cell cluster quantitation

Liver sections stained for CD45 by immunofluorescence were viewed using Leica DM RBE Fluorescence Microscope (Leica Microsystems) and photographed using Leica DFC 500 camera (Leica Microsystems) in random fields of view (FOV) (n = 3–10). Fluorescent cells were quantified blind using Image-J (National Institute of Mental Health, MD, USA). Cell clusters were defined as greater than five cells in contact.

Statistics

Statistical analysis was performed using Prism 6 (GraphPad, San Diego, USA). Mann-Whitney U t-test was performed to compare against control unless otherwise specified. Significance was accepted at $p<0.05$. Data are shown as mean ± SEM. As indicated some data are expressed as fold change from control.

Results

CD147 gene expression increases in the liver during injury

We have previously observed higher CD147 expression in *p*rimary *b*iliary *c*holangitis (PBC), *p*rimary *s*clerosing *c*holangitis (PSC) and *h*epatitis *C v*irus (HCV)-induced liver injury in patients [12,55]. We chose to investigate the expression of CD147 in a TAA-induced mouse model of liver injury to further establish the source and function of CD147 in liver injury. During the development of TAA-induced liver injury, we observed a progressive increase in the expression of CD147 mRNA in whole liver tissue (7-fold) (Fig 1A). When hepatocytes and leukocytes were analysed separately, a significant increase in CD147 mRNA expression was observed in leukocytes (30-fold) (Fig 1B) and minimal CD147 upregulation was observed on hepatocytes (2-fold) (Fig 1B). This data shows that CD147 expression is upregulated in a mouse model of liver injury and has predominantly increased expression on leukocytes. This demonstrates that while hepatocytes are the dominant cell type in liver tissue, it is the less abundant leukocytes that have the greatest contribution to CD147 upregulation in whole liver, seen by the larger fold-change in CD147 expression on leukocytes compared to hepatocytes (30-fold vs. 2-fold for leukocytes and hepatocytes, respectively). Further, we examined leukocyte CD147 expression in blood, liver and spleen, and demonstrated an increase from control to 20 weeks in circulating and intrahepatic leukocytes (Fig 1C).

CD147 surface expression increases on liver leukocyte subsets during injury

We next characterized the expression of CD147 on various leukocyte subsets during the course of liver injury (Fig 2). Eight colour flow cytometry was utilized to gate liver $CD4^+$ T cells, $CD8^+$ T cells, B cells, NK cells, NKT cells, eosinophils, neutrophils and, macrophages. In

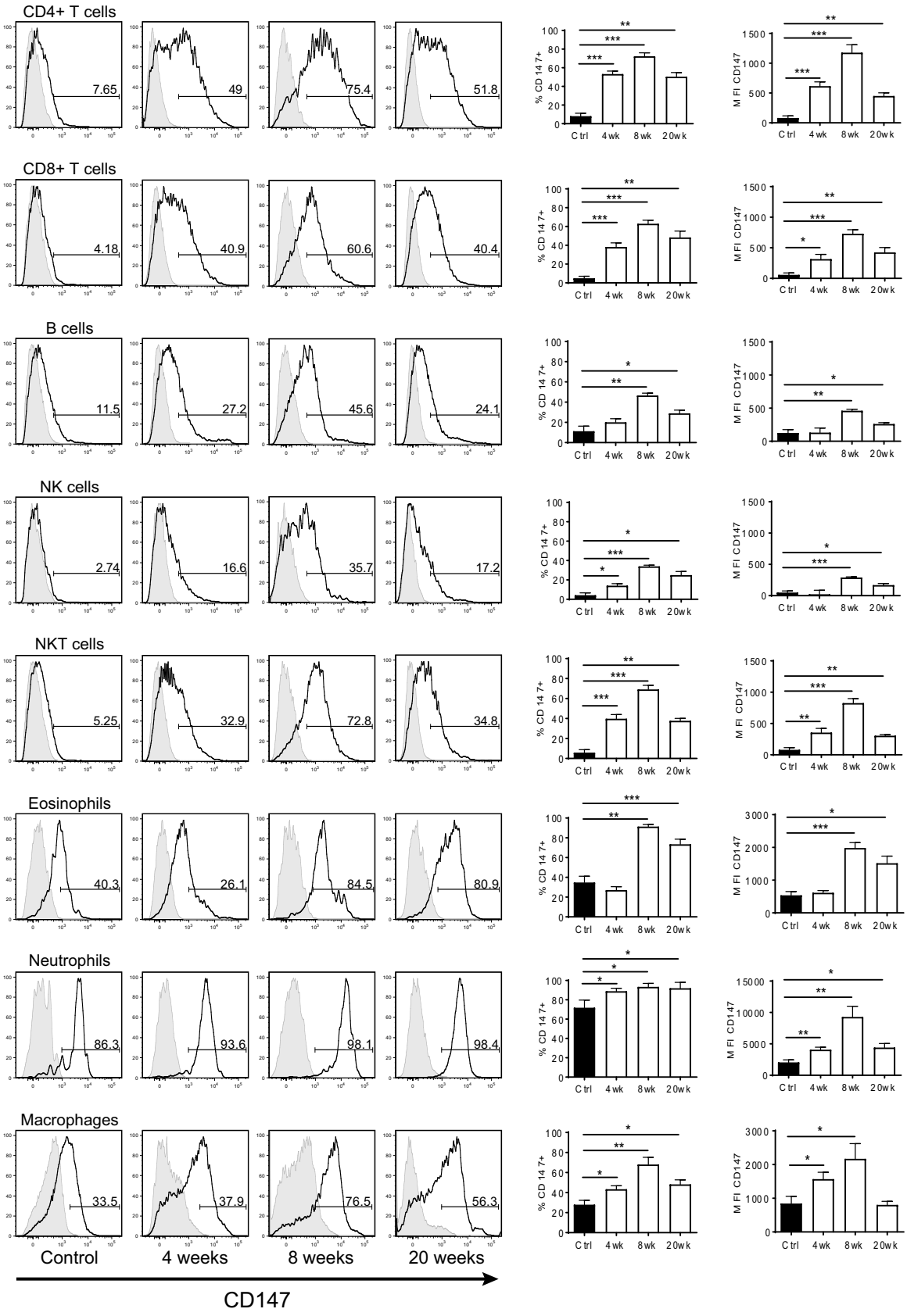
CD4+ T cells
7.65
49
75.4
51.8
CD8+ T cells
4.18
40.9
60.6
40.4
B cells
11.5
27.2
45.6
24.1
NK cells
2.74
16.6
35.7
17.2
NKT cells
5.25
32.9
72.8
34.8
Eosinophils
40.3
26.1
84.5
80.9
Neutrophils
86.3
93.6
98.1
98.4
Macrophages
33.5
37.9
76.5
56.3
Control
4 weeks
8 weeks
20 weeks
CD147
% CD 14 7+
M FI CD147
C trl
4 wk
8 wk
20 wk

Fig 2. CD147 surface expression on leukocyte subsets isolated from livers in progressive liver injury. Flow cytometry was performed on liver leukocytes from control and TAA-treated mice. Each leukocyte subset was analysed for expression of CD147 and data recorded as the percentage of cells positive for CD147 (%CD147+) or mean fluorescence intensity (MFI). Representative histogram plots are shown for each subset, where the black histogram represents the indicated liver subset and grey histogram indicates isotype control. Bar graphs represent mean ± SEM Mann-Whitney test was performed to assess significance from control where * $p<0.05$, ** $p<0.01$, *** $p<0.001$ (n = 5–8 per group).

https://doi.org/10.1371/journal.pone.0215557.g002

untreated controls, leukocytes expressed minimal CD147 with the exception of macrophages, neutrophils and eosinophils, which all had high basal levels of CD147. CD147 expression increased on all liver leukocytes, with peak expression at 8 weeks of injury. Interestingly, as liver injury progressed, we observed a significant loss of NKT cells and macrophages, and a significant increase of $CD8^+$ T cells, eosinophils and neutrophils from the liver.

To establish whether similar CD147 expression patterns were occurring in an extrahepatic lymphoid organ, the spleen was also analysed by flow cytometry in the same manner as

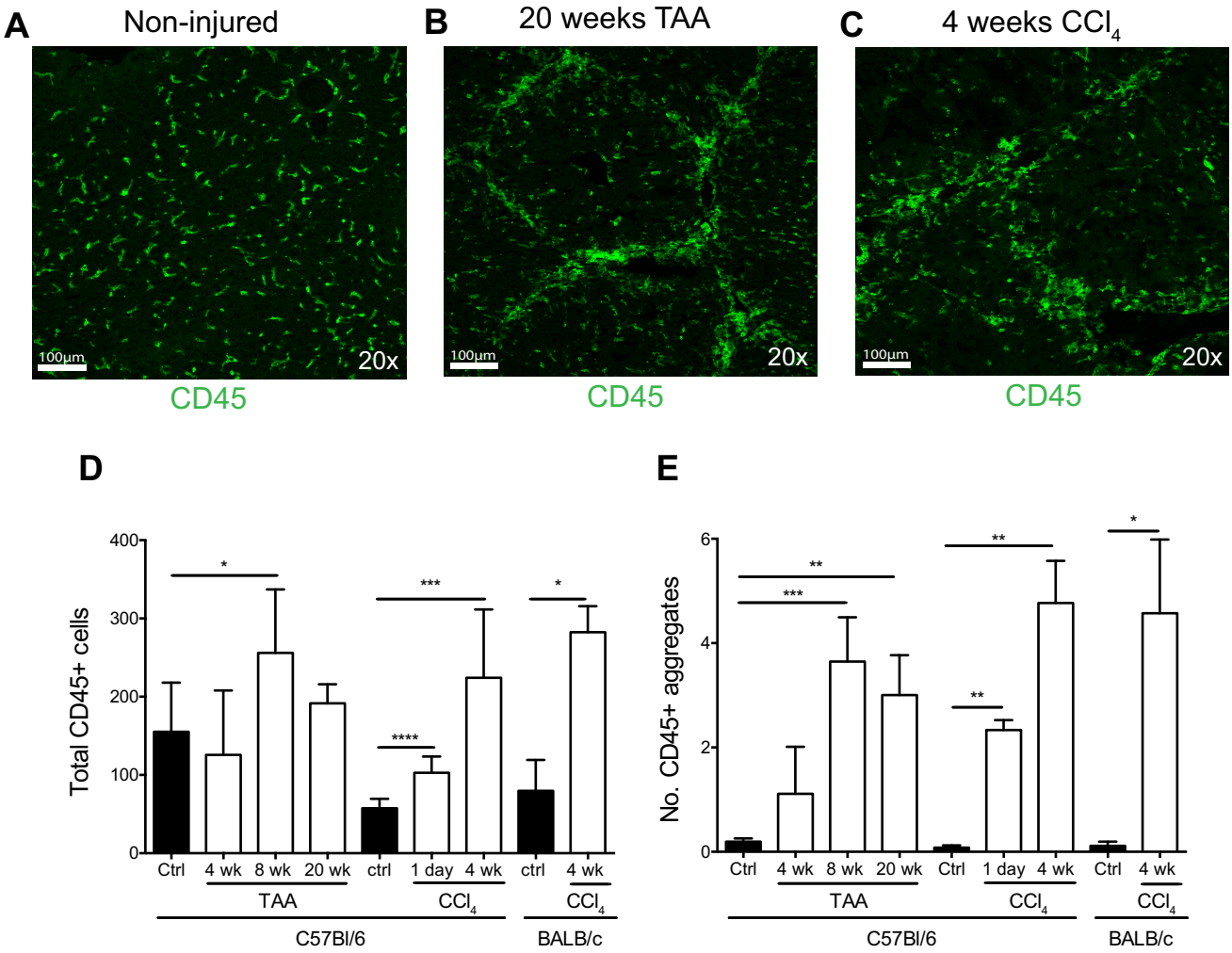

Fig 3. Aggregation of immune cell infiltrate in mouse liver injury. Inflammatory infiltrates in liver tissue of control, 4, 8 and 20-week TAA-treated C57Bl/6 mice and control, 1 day and 4 weeks CCl_4 treated C57Bl/6 and BALB/c mice. Representative images of CD45 stained liver sections from (A) non-injured control; (B) 20-week TAA and (C) 4 week CCl_4 treated mice. Scale represents 100μM. (D) Total $CD45^+$ cells were quantified per field of view with 4–10 fields counted per section. Bars represent mean+SEM. (E) Immune cell aggregates were quantified (≥5 $CD45^+$ cells per cluster) per field of view (FOV). Bars represent mean+SEM. Mann-Whitney test was performed to assess significance from control where * $p<0.05$, ** $p<0.01$, *** $p<0.001$, **** $p<0.0001$ (n = 5–8 per group).

https://doi.org/10.1371/journal.pone.0215557.g003

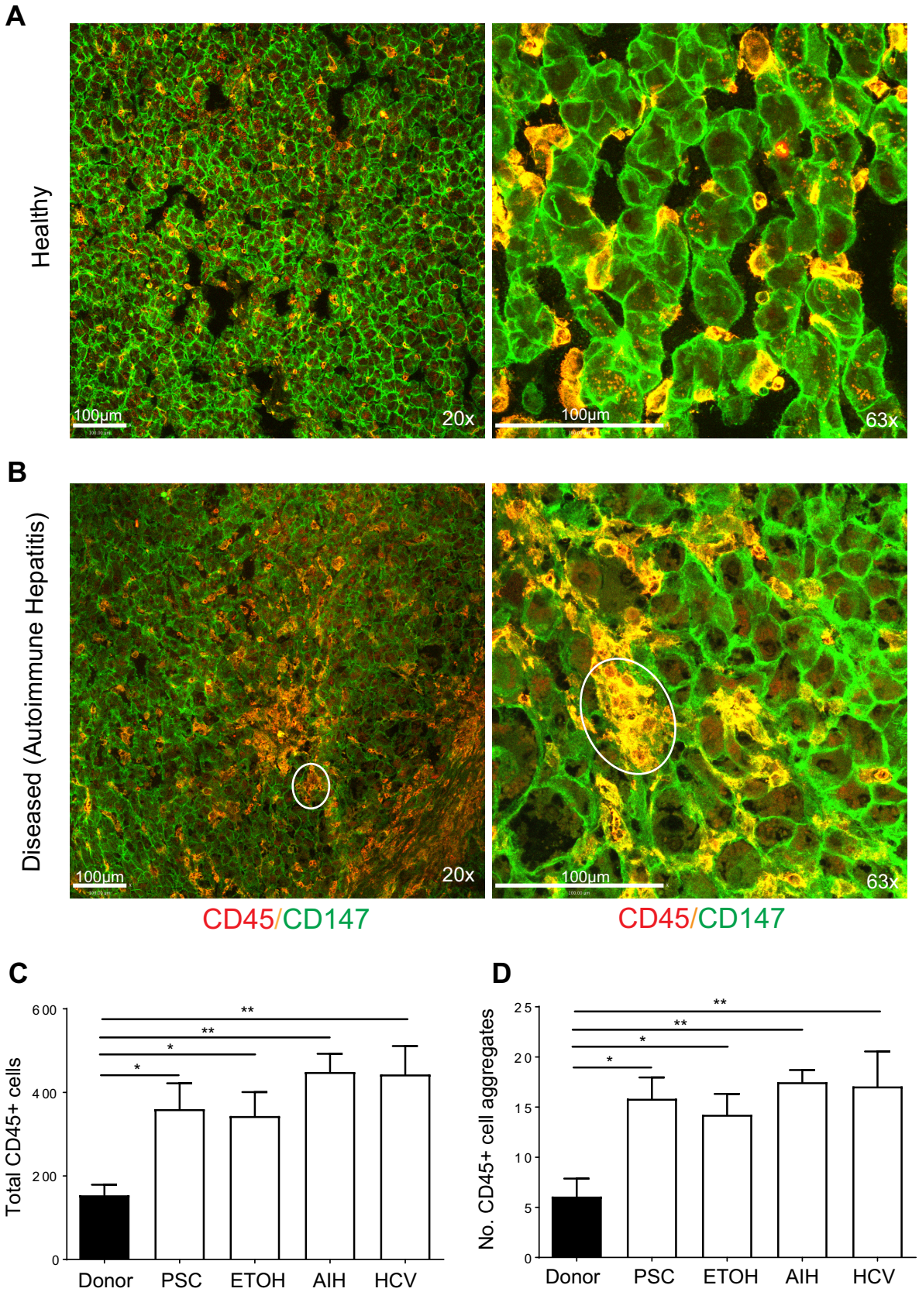
A
Healthy
100μm
20x
100μm
63x
B
Diseased (Autoimmune Hepatitis)
100μm
20x
100μm
63x
CD45/CD147
CD45/CD147
C
Total CD45+ cells
600
400
200
0
**
**
*
*
Donor
PSC
ETOH
AIH
HCV
D
No. CD45+ cell aggregates
25
20
15
10
5
0
**
**
*
*
Donor
PSC
ETOH
AIH
HCV

Fig 4. Aggregation of CD147+ immune cells in diseased liver. Representative images of liver sections stained with CD45 (red) and CD147 (green) from (A) healthy control and (B) diseased patient liver (autoimmune hepatitis) on either a 20x (left panels) or 63x (right panels) objective. Yellow indicates co-expression of CD147 and CD45. Scale bar represents 100μM. Quantification of (C) total CD45+ cells and (D) immune aggregates in healthy, PSC, EtOH, AIH and HCV livers. Bars represent mean+SEM. Unpaired t-test was performed to assess significance from control where $^{*}p<0.05$ and $^{**}p<0.01$ (n = 4–15 per group). Donor = healthy control liver, PSC = primary sclerosing cholangitis, ETOH = alcohol-induced liver damage, AIH = Autoimmune hepatitis, HCV = hepatitis C virus liver injury.

https://doi.org/10.1371/journal.pone.0215557.g004

described above. The observed trend was true for all sub-populations examined, with the exception of NK cells, which showed equally high expression at both 8 and 20 weeks. Interestingly, some splenic sub-populations showed a similar trend, however, CD147 expression was not nearly as high as in the liver and no values were significantly up-regulated compared to untreated mice. Within each treatment group, CD147 expression levels were relatively similar amongst all leukocyte subsets, with the exception of macrophages, which displayed expression levels up to 6-fold higher than any other cell type. B cells and NK cells showed the lowest relative expression of CD147, displaying levels half that of the T cell subsets (Fig 2).

Aggregation of lymphocytes during liver injury in mouse models

To determine how lymphocytes localized during chronic liver injury, CD45 staining was conducted on a range of injury models including, TAA treatment in C57Bl/6, CCl_4 in C57Bl/6 and CCl_4 in BALB/c mice (Fig 3). In uninjured control livers, lymphocytes dispersed evenly within the liver tissue (Fig 3A). In contrast, in both TAA (Fig 3B) and CCl_4 (Fig 3C) injury models, not only were total $CD45^+$ cells numbers elevated (Fig 3D) but $CD45^+$ cells were found to aggregate (defined as >5 $CD45^+$ cells in contact). Importantly the majority of aggregation occurred around portal triads where fibrosis first appears. Peak infiltrate was observed after 8 weeks of TAA and 4 weeks of CCl_4, which correlated with peak immune cell aggregation (Fig 3E). Thus, injury is shown to increase immune cell infiltrate and immune cell aggregation.

Apoptosis and proliferation within aggregates were assessed by cleaved caspase-3 and Ki-67, respectively (S1 Fig). This was assessed in both normal and injured liver tissue. In C57Bl/6 mice, after 4 weeks of CCl_4 administration compared to untreated animals, apoptosis went from being most undetected to occasionally seen, which was a significant increase ($p = 0.05$), but no significant change in proliferation was observed ($p = 0.08$). This is consistent with other publications [56,57].

Aggregation of lymphocytes in injured human liver

To confirm that immune cell expression of CD147 and immune cell aggregation was not exclusive to mouse models we examined human liver tissue from healthy donors (Fig 4A) and patients with PSC, alcohol-induced liver damage (EtOH), *a*uto*i*mmune *h*epatitis (AIH) and HCV (Fig 4B). Interestingly, we observed CD147 expression on hepatocytes and all CD45+ immune cells in both healthy and injured livers. Total $CD45^+$ immune cells were significantly increased in diseased liver tissue, irrespective of whether the disease was immune-mediated (AIH, PSC, HCV) or not (EtOH) (Fig 4C). Inflammatory cells were shown to aggregate with liver injury (Fig 4B) and significantly more immune aggregates were observed in diseased livers compared to healthy donor livers (Fig 4D). In healthy donors, although $CD45^+$ cells expressed some level of CD147, immune cells did not aggregate. Therefore, this data confirms that in diseased human liver, CD147 is expressed on $CD45^+$ immune cell infiltrate and immune cells aggregate during disease.

CD147-dependent leukocyte aggregation in liver injury

To determine whether CD147 was important for the formation of immune cell aggregates, the effects of anti-CD147 intervention were studied in CCl_4 induced liver injury models in both

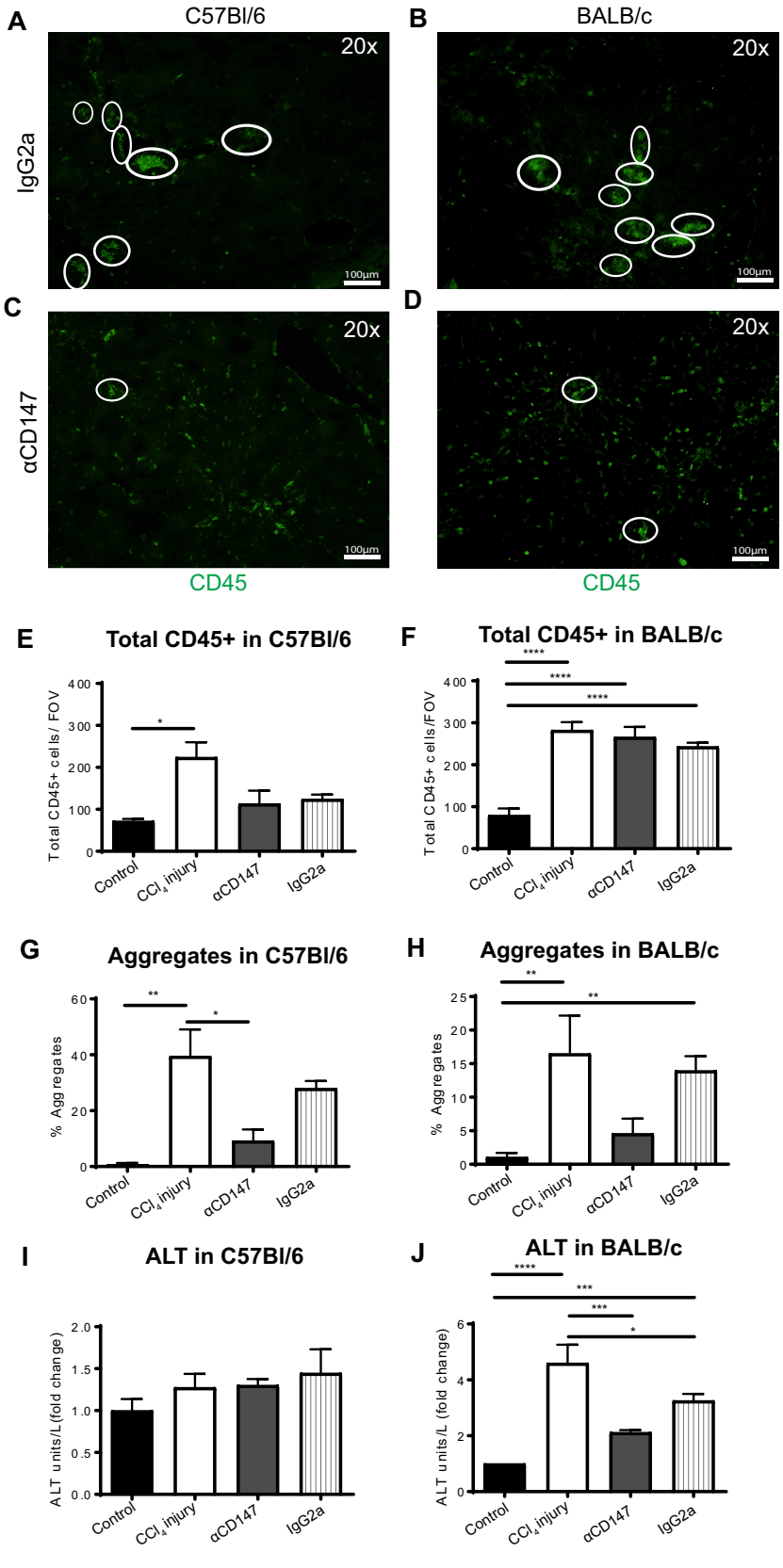
A
C57Bl/6
B
BALB/c
20x
IgG2a
αCD147
C
D
CD45
E
Total CD45+ in C57Bl/6
F
Total CD45+ in BALB/c
Total CD45+ cells/ FOV
Control
CCl4 injury
αCD147
IgG2a
G
Aggregates in C57Bl/6
H
Aggregates in BALB/c
% Aggregates
I
ALT in C57Bl/6
J
ALT in BALB/c
ALT units/L (fold change)

Fig 5. CD147 blockade prevents immune cell aggregation in liver injury. Anti-CD147 antibody intervention in CCl_4 induced liver injury in C57Bl/6 (left panels) or BALB/c (right panels) mice. CD45+ leukocytes were stained in frozen tissue sections in control, treatment (CCl_4), treatment with anti-CD147 antibody intervention, or treatment with IgG2a isotype antibody controls. Representative immunofluorescent images of $CD45^+$ clusters defined as ≥5 cells per cluster (white circles) are shown in C57Bl/6 (A) and BALB/c mice (B) treated with IgG2a. Representative immunofluorescence images of $CD45^+$ clusters following αCD147 intervention in C57Bl/6 (C) and BALB/c (D) mice. Total $CD45^+$ leukocytes in C57Bl/6 (E) and BALB/c (F) mice. (G) Percentage of $CD45^+$ cells in aggregates for each treatment group in C57Bl/6 (G) and BALB/c (H) mice. ALT levels (U/L) as a measure of liver damage in C57Bl/6 (I) and BALB/c (J) mice, calculated as a fold change from control. Bar graphs represent mean ± SEM. Mann-Whitney test was performed to assess significance from control where * $p<0.05$, ** $p<0.01$, *** $p<0.001$ (n = 5–8 per group). Control = untreated, CCl_4 injury = injury alone, αCD147 = anti-CD147 mAb in CCl_4 injury, IgG2a = Isotype mAb control in CCl_4 injury.

https://doi.org/10.1371/journal.pone.0215557.g005

C57Bl/6 and BALB/c mice. Anti-CD147 did not significantly reduce the number of $CD45^+$ cells in the liver (Fig 5E and 5F). The percentage of immune cells that formed immune cell aggregates was reduced with anti-CD147 intervention in both mouse backgrounds (Fig 5G and 5H). In C57Bl/6 mice, there was a non-significant (<1.5-fold) increase in ALT with liver injury and no significant change was seen with anti-CD147 intervention (Fig 5I). However, in BALB/c mice, which are known to be more sensitive than C57Bl/6 mice to hepatotoxins such as CCl_4 [58], a significant increase in ALT was observed in liver injury compared to control and anti-CD147 intervention significantly reduced serum ALT levels (Fig 5J). Thus, CD147 inhibition appeared to significantly reduce the formation of immune cell aggregates and reduce liver injury.

Specific leukocyte subsets within aggregates

We have just shown that anti-CD147 intervention reduces the percentage of immune cells in aggregates. To determine what inflammatory cells were aggregating in CCl_4 induced liver injury and to determine whether this is altered during anti-CD147 intervention, mouse liver samples were immunostained with CD45, F4/80, B220, Gr1 and CD3. $F4/80^+$ Macrophages, $B220^+$ B cells, $Gr1^+$ granulocytes and $CD3^+$ T cells (including NKT cells) were all found in aggregates during liver injury (Fig 6). After anti-CD147 treatment, we observed a decrease in the number of aggregates with at least one $F4/80^+$, $B220^+$ and $CD3^+$ cell. The number of $Gr1^+$ cells in aggregates was not altered after anti-CD147 treatment (Fig 6). Thus, anti-CD147 intervention was shown to target specific immune cell subsets and reduce immune cell aggregation.

Discussion

This study has demonstrated that with progressive inflammation-associated tissue injury, immune cells aggregate and directly contribute to the severity of the injury. Our novel discovery is that with liver injury, CD147 is principally upregulated on the surface of leukocytes and mediates cell-cell aggregation that determines the extent of liver injury. We have also shown that if CD147 is blocked with a mAb, then the numbers of infiltrating $CD45^+$ cells in the liver remain unchanged but leukocytes are no longer found in aggregates. Importantly, we have already reported that there is a significant reduction in liver injury seen with anti-CD147 mAb [15]. Further, CD147-mediated leukocyte aggregation appears to cause (or significantly exacerbate) injury as aggregate formation proceeds the development of significant fibrosis [15]. Therefore, this is not just a reduction in aggregation and inflammatory markers (AST/ALT) but also a reduction in resultant fibrosis.

All intrahepatic leukocyte subpopulations ($CD4^+$, $CD8^+$, NK, B-cell and macrophages) rapidly increase CD147 surface protein and total mRNA expression during liver injury. Therefore, this data shows that following liver injury, circulating and intrahepatic leukocytes increase

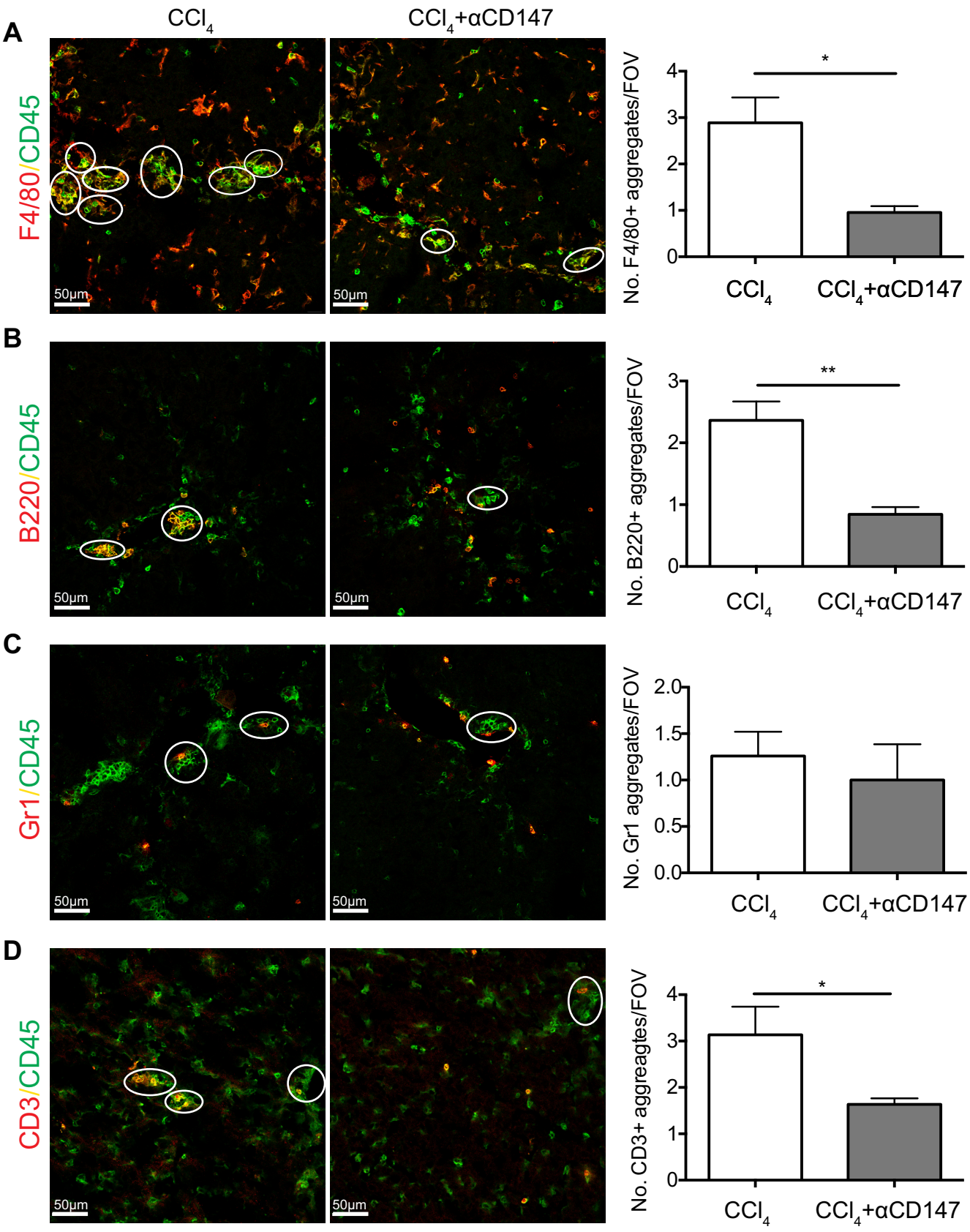
A
CCl4
CCl4+αCD147
F4/80/CD45
50μm
50μm
No. F4/80+ aggregates/FOV
*
CCl4
CCl4+αCD147
B
B220/CD45
50μm
50μm
No. B220+ aggregates/FOV
**
CCl4
CCl4+αCD147
C
Gr1/CD45
50μm
50μm
No. Gr1 aggregates/FOV
CCl4
CCl4+αCD147
D
CD3/CD45
50μm
50μm
No. CD3+ aggreagtes/FOV
*
CCl4
CCl4+αCD147

Fig 6. Anti-CD147 intervention reduces aggregation of macrophages, B cells, T cells and granulocytes during liver injury. CCl_4 treated C57Bl/6 mice liver tissue was stained for CD45 colocalisation with (A) F4/80, (B) B220, (C) Gr1 or (D) CD3, to identify immune subset specific aggregates. Representative images (left panel) and quantified immune cell-specific aggregates (right panel; calculated as at least one cell of interest per aggregate) in mice treated with CCl_4 alone or CCl_4 in conjunction with anti-CD147 intervention. Bar graphs represent mean ± SEM. Mann-Whitney test was performed to assess significance from control where * $p<0.05$, $^{**}p<0.01$ (n = 5–7 per group). CCl_4 = injury alone, αCD147 = anti-CD147 in CCl_4 injury.

https://doi.org/10.1371/journal.pone.0215557.g006

CD147 expression. Subsequently, it has been shown leukocytes undergo activation [59] and form aggregates that contribute to injury. It is unknown if leukocyte activation occurs concurrent or prior to aggregation. The recruitment of inflammatory cells from the periphery to sites of liver injury is important in the pathogenesis of liver injury [59] but its relationship to aggregation and dependence on CD147 expression was unrecognised. Based on these results, CD147 is likely pivotal to the development of inflammation in liver injury, partly through the previously unrecognized role in leukocyte aggregate formation.

In liver injury, anti-CD147 intervention leads to a reduction in immune cell aggregation, characterised by a reduction in serum transaminases and total tissue MMP activity [15]. Importantly, there is no significant change in the total number of $CD45^{+}$ cells infiltrating the liver. This suggests that the cells are not proliferating to form clusters but rather they aggregate with injury. Further, we have shown that the clusters that diminish with anti-CD147 intervention in injury contain B-cells (B220) and macrophages/Kupffer cells (F4/80), whereas the isotype antibody controls have the same phenotype as wild-type animals. Importantly, we have shown these leukocyte clusters form in progressive human liver injury, irrespective of disease etiology.

CD147 has a number of binding interactions. The CD147 binding partners; α3β1, α6β1, CD44, LFA-1, ICAM-1, sydnedcan-1 and hyaluronan, all have known roles in immune cell retention at sites of inflammation. The functional significance of CD147 protein binding interactions in the aggregation phenotype is unknown but likely pivotal and clearly needs to be determined. Multiple proteins are known membrane-binding partners of CD147 (see Background) [29,30,38–40]. Further, many of the CD147 complex proteins are found on leukocytes and/or have known roles in leukocyte retention at sites of inflammation (including CD98 [38], β1-integrin [38], CD43 [60], LFA-1 [28,43,60], ICAM-1 [43], sydnecan-1 [28,60], and hyaluronan [39,61]). Additionally, CD147 through interactions with CD98 [38,39] and/or β1-integrin [38] is known to mediate homotypic cell clustering of leukocytes. Therefore, CD98 [38,39], β1-integrin [38], LFA-1 [28,43,60] and ICAM-1 [43] are the most promising protein binding partners to study that are likely involved in the aggregation phenotype.

Therefore, we have identified CD147 as a potential therapeutic target to minimize exacerbation of liver injury via reduction of leukocyte aggregate accumulations in the liver tissue. Further work is required to determine the role of CD147 in liver fibrogenesis resultant from persistent inflammatory insult.

Supporting information

S1 Fig. Apoptosis and proliferation within immune cell aggregates. In CCl_4 treated C57Bl/6 mice and healthy controls, liver tissue was stained with cleaved caspase-3 and Ki-67 to assess apoptosis and proliferation within aggregates, respectively. (A) Representative images of apoptosis (left panels) and proliferation (right panels) from healthy control mice (top panels) and CCl_4 treated mice (bottom panels). (B) The number of positive events per frame where bar graphs represent mean ± SEM Mann-Whitney test was performed to assess significance from control. (n = 5–7 per group).
(EPS)

S1 Table. Changes in mouse weights following hepatotoxin treatment or antibody intervention. Start and end mouse body weights for C57Bl/6 and Balb/c mice following hepatotoxin treatment and/or antibody intervention. Data are expressed as mean ± SEM. Mann-Whitney test was performed to assess significance from control where *** $p<0.001$ vs H_2O Control, **** $p<0.0001$ vs H_2O Control. H_2O control = H_2O only, PO control = PO only, CCl_4 injury = CCl_4 injury alone, TAA = TAA injury alone, αCD147 = anti-CD147 mAb in CCl_4 injury, IgG2a = Isotype mAb control in CCl_4 injury.
(DOCX)

Author Contributions

Conceptualization: Christine Yee, David G. Bowen, Fiona J. Warner, Geoffrey W. McCaughan, Susan V. McLennan, Nicholas A. Shackel.

Data curation: Christine Yee, Nathan M. Main, Alexandra Terry, Igor Stevanovski, Nicholas A. Shackel.

Formal analysis: Christine Yee, Nathan M. Main, Alexandra Terry, Igor Stevanovski, Nicholas A. Shackel.

Funding acquisition: Susan V. McLennan, Nicholas A. Shackel.

Investigation: Christine Yee, Nathan M. Main, Alexandra Terry, Igor Stevanovski, Annette Maczurek, Alison J. Morgan, Sarah Calabro, Alison J. Potter, Tina L. Iemma.

Methodology: Christine Yee, Nathan M. Main, Alexandra Terry, Igor Stevanovski.

Project administration: Christine Yee, Nathan M. Main, Susan V. McLennan, Nicholas A. Shackel.

Resources: Nicholas A. Shackel.

Supervision: Fiona J. Warner, Geoffrey W. McCaughan, Susan V. McLennan, Nicholas A. Shackel.

Writing – original draft: Christine Yee, Nathan M. Main, Alexandra Terry, Igor Stevanovski, Fiona J. Warner, Nicholas A. Shackel.

Writing – review & editing: Christine Yee, Nathan M. Main, Alexandra Terry, David G. Bowen, Golo Ahlenstiel, Nicholas A. Shackel.

References

1. Friedman SL. Molecular regulation of hepatic fibrosis, an integrated cellular response to tissue injury. J Biol Chem. 2000; 275(4):2247–50. https://doi.org/10.1074/jbc.275.4.2247 PMID: 10644669.
2. Riordan SM, Skinner N, Nagree A, McCallum H, McIver CJ, Kurtovic J, et al. Peripheral blood mononuclear cell expression of toll-like receptors and relation to cytokine levels in cirrhosis. Hepatology. 2003; 37(5):1154–64. Epub 2003/04/30. https://doi.org/10.1053/jhep.2003.50180 PMID: 12717397.
3. Preiss S, Thompson A, Chen X, Rodgers S, Markovska V, Desmond P, et al. Characterization of the innate immune signalling pathways in hepatocyte cell lines. J Viral Hepat. 2008; 15(12):888–900. Epub 2008/08/05. https://doi.org/10.1111/j.1365-2893.2008.01001.x PMID: 18673429.
4. Testro AG, Visvanathan K. Toll-like receptors and their role in gastrointestinal disease. J Gastroenterol Hepatol. 2009; 24(6):943–54. Epub 2009/07/30. https://doi.org/10.1111/j.1440-1746.2009.05854.x PMID: 19638078.
5. Berzsenyi MD, Roberts SK, Preiss S, Woollard DJ, Beard MR, Skinner NA, et al. Hepatic TLR2 & TLR4 expression correlates with hepatic inflammation and TNF-alpha in HCV & HCV/HIV infection. J Viral Hepat. 2011; 18(12):852–60. Epub 2010/11/06. https://doi.org/10.1111/j.1365-2893.2010.01390.x PMID: 21050341.

6. Testro AG, Gow PJ, Angus PW, Wongseelashote S, Skinner N, Markovska V, et al. Effects of antibiotics on expression and function of Toll-like receptors 2 and 4 on mononuclear cells in patients with advanced cirrhosis. J Hepatol. 2010; 52(2):199–205. Epub 2009/12/17. https://doi.org/10.1016/j.jhep.2009.11.006 PMID: 20006396.
7. Bowen DG, Zen M, Holz L, Davis T, McCaughan GW, Bertolino P. The site of primary T cell activation is a determinant of the balance between intrahepatic tolerance and immunity. J Clin Invest. 2004; 114 (5):701–12. Epub 2004/09/03. https://doi.org/10.1172/JCI21593 PMID: 15343389; PubMed Central PMCID: PMCPMC514586.
8. Holz LE, Warren A, Le Couteur DG, Bowen DG, Bertolino P. CD8+ T cell tolerance following antigen recognition on hepatocytes. J Autoimmun. 2010; 34(1):15–22. Epub 2009/09/12. https://doi.org/10.1016/j.jaut.2009.08.005 PMID: 19744829.
9. Warren A, Le Couteur DG, Fraser R, Bowen DG, McCaughan GW, Bertolino P. T lymphocytes interact with hepatocytes through fenestrations in murine liver sinusoidal endothelial cells. Hepatology. 2006; 44 (5):1182–90. Epub 2006/10/24. https://doi.org/10.1002/hep.21378 PMID: 17058232.
10. Corpechot C, Barbu V, Wendum D, Kinnman N, Rey C, Poupon R, et al. Hypoxia-induced VEGF and collagen I expressions are associated with angiogenesis and fibrogenesis in experimental cirrhosis. Hepatology. 2002; 35(5):1010–21. Epub 2002/05/01. https://doi.org/10.1053/jhep.2002.32524 PMID: 11981751.
11. Damsker JM, Okwumabua I, Pushkarsky T, Arora K, Bukrinsky MI, Constant SL. Targeting the chemotactic function of CD147 reduces collagen-induced arthritis. Immunology. 2009; 126(1):55–62. Epub 2008/06/19. https://doi.org/10.1111/j.1365-2567.2008.02877.x PMID: 18557953; PubMed Central PMCID: PMCPMC2632695.
12. Shackel NA, McGuinness PH, Abbott CA, Gorrell MD, McCaughan GW. Identification of novel molecules and pathogenic pathways in primary biliary cirrhosis: cDNA array analysis of intrahepatic differential gene expression. Gut. 2001; 49(4):565–76. Epub 2001/09/18. https://doi.org/10.1136/gut.49.4.565 PMID: 11559656; PubMed Central PMCID: PMCPMC1728487.
13. Shackel NA, McGuinness PH, Abbott CA, Gorrell MD, McCaughan GW. Insights into the Pathobiology of Hepatitis C Virus Associated Cirrhosis: Analysis of Intrahepatic Differential Gene Expression. American Journal of Pathology. 2002; 160(2):641–54. https://doi.org/10.1016/S0002-9440(10)64884-5 PMID: 11839585
14. Shackel NA, McGuinness PH, Abbott CA, Gorrell MD, McCaughan GW. Novel differential gene expression in human cirrhosis detected by suppression subtractive hybridization. Hepatology. 2003; 38 (3):577–88. Epub 2003/08/27. https://doi.org/10.1053/jhep.2003.50376 PMID: 12939584.
15. Calabro SR, Maczurek AE, Morgan AJ, Tu T, Wen VW, Yee C, et al. Hepatocyte produced matrix metalloproteinases are regulated by CD147 in liver fibrogenesis. PloS one. 2014; 9(7):e90571. Epub 2014/07/31. https://doi.org/10.1371/journal.pone.0090571 PMID: 25076423; PubMed Central PMCID: PMCPMC4116334.
16. Kirschner K, Bisswanger H. Multifunctional proteins. Annu Rev Biochem. 1976; 45:143–66. Epub 1976/01/01. https://doi.org/10.1146/annurev.bi.45.070176.001043 PMID: 786148.
17. Jeffery CJ. Multifunctional proteins: examples of gene sharing. Ann Med. 2003; 35(1):28–35. Epub 2003/04/16. PMID: 12693610.
18. Jiang J, Casalegno-Garduno R, Chen H, Schmitt A, Schmitt M, Maxwell CA. Multifunctional proteins bridge mitosis with motility and cancer with inflammation and arthritis. ScientificWorldJournal. 2010; 10:1244–57. Epub 2010/07/06. https://doi.org/10.1100/tsw.2010.141 PMID: 20602082.
19. Ravindran S, George A. Multifunctional ECM proteins in bone and teeth. Exp Cell Res. 2014; 325 (2):148–54. Epub 2014/02/04. https://doi.org/10.1016/j.yexcr.2014.01.018 PMID: 24486446; PubMed Central PMCID: PMCPMC4072740.
20. Chapple CE, Robisson B, Spinelli L, Guien C, Becker E, Brun C. Extreme multifunctional proteins identified from a human protein interaction network. Nat Commun. 2015; 6:7412. Epub 2015/06/10. https://doi.org/10.1038/ncomms8412 PMID: 26054620; PubMed Central PMCID: PMCPMC4468855.
21. Yurchenko V, Constant S, Bukrinsky M. Dealing with the family: CD147 interactions with cyclophilins. Immunology. 2006; 117(3):301–9. Epub 2006/02/16. https://doi.org/10.1111/j.1365-2567.2005.02316.x PMID: 16476049; PubMed Central PMCID: PMCPMC1782239.
22. Toole BP. Emmprin (CD147), a cell surface regulator of matrix metalloproteinase production and function. Current Topics in Developmental Biology. 2003; 54:371–89. PMID: 12696756.
23. Bao W, Min D, Twigg SM, Shackel NA, Warner FJ, Yue DK, et al. Monocyte CD147 is induced by advanced glycation end products and high glucose concentration: possible role in diabetic complications. Am J Physiol Cell Physiol. 2010; 299(5):C1212–9. Epub 2010/09/03. https://doi.org/10.1152/ajpcell.00228.2010 PMID: 20810913.

24. Lim M, Martinez T, Jablons D, Cameron R, Guo H, Toole B, et al. Tumor-derived EMMPRIN (extracellular matrix metalloproteinase inducer) stimulates collagenase transcription through MAPK p38. FEBS Lett. 1998; 441(1):88–92. Epub 1999/01/07. https://doi.org/10.1016/s0014-5793(98)01474-4 PMID: 9877171.

25. Huang Z, Wang C, Wei L, Wang J, Fan Y, Wang L, et al. Resveratrol inhibits EMMPRIN expression via P38 and ERK1/2 pathways in PMA-induced THP-1 cells. Biochemical and biophysical research communications. 2008; 374(3):517–21. Epub 2008/07/24. https://doi.org/10.1016/j.bbrc.2008.07.058 PMID: 18647594.

26. Fan Y, Meng S, Wang Y, Cao J, Wang C. Visfatin/PBEF/Nampt induces EMMPRIN and MMP-9 production in macrophages via the NAMPT-MAPK (p38, ERK1/2)-NF-kappaB signaling pathway. Int J Mol Med. 2011; 27(4):607–15. Epub 2011/02/18. https://doi.org/10.3892/ijmm.2011.621 PMID: 21327328.

27. Kim JY, Kim H, Suk K, Lee WH. Activation of CD147 with cyclophilin a induces the expression of IFITM1 through ERK and PI3K in THP-1 cells. Mediators Inflamm. 2010; 2010:821940. Epub 2010/09/18. https://doi.org/10.1155/2010/821940 PMID: 20847954; PubMed Central PMCID: PMC2935166.

28. Yurchenko V, Constant S, Eisenmesser E, Bukrinsky M. Cyclophilin-CD147 interactions: a new target for anti-inflammatory therapeutics. Clin Exp Immunol. 2010; 160(3):305–17. Epub 2010/03/30. https://doi.org/10.1111/j.1365-2249.2010.04115.x PMID: 20345978; PubMed Central PMCID: PMCPMC2883100.

29. Yurchenko V, O'Connor M, Dai WW, Guo H, Toole B, Sherry B, et al. CD147 is a signaling receptor for cyclophilin B. Biochemical and biophysical research communications. 2001; 288(4):786–8. Epub 2001/11/02. https://doi.org/10.1006/bbrc.2001.5847 PMID: 11688976.

30. Yurchenko V, Zybarth G, O'Connor M, Dai WW, Franchin G, Hao T, et al. Active site residues of cyclophilin A are crucial for its signaling activity via CD147. J Biol Chem. 2002; 277(25):22959–65. Epub 2002/04/12. https://doi.org/10.1074/jbc.M201593200 M201593200 [pii]. PMID: 11943775.

31. Zhu P, Lu N, Shi ZG, Zhou J, Wu ZB, Yang Y, et al. CD147 overexpression on synoviocytes in rheumatoid arthritis enhances matrix metalloproteinase production and invasiveness of synoviocytes. Arthritis Res Ther. 2006; 8(2):R44. Epub 2006/03/02. https://doi.org/10.1186/ar1899 PMID: 16507143; PubMed Central PMCID: PMC1526600.

32. Treese C, Mittag A, Lange F, Tarnok A, Loesche A, Emmrich F, et al. Characterization of fibroblasts responsible for cartilage destruction in arthritis. Cytometry A. 2008; 73(4):351–60. Epub 2008/03/01. https://doi.org/10.1002/cyto.a.20532 PMID: 18307273.

33. Wang CH, Dai JY, Wang L, Jia JF, Zheng ZH, Ding J, et al. Expression of CD147 (EMMPRIN) on neutrophils in rheumatoid arthritis enhances chemotaxis, matrix metalloproteinase production and invasiveness of synoviocytes. J Cell Mol Med. 2010. Epub 2010/05/12. JCMM1084 [pii] https://doi.org/10.1111/j.1582-4934.2010.01084.x PMID: 20455995.

34. Agrawal SM, Silva C, Tourtellotte WW, Yong VW. EMMPRIN: a novel regulator of leukocyte transmigration into the CNS in multiple sclerosis and experimental autoimmune encephalomyelitis. The Journal of neuroscience: the official journal of the Society for Neuroscience. 2011; 31(2):669–77. Epub 2011/01/14. https://doi.org/10.1523/JNEUROSCI.3659-10.2011 PMID: 21228176.

35. Betsuyaku T, Kadomatsu K, Griffin GL, Muramatsu T, Senior RM. Increased basigin in bleomycin-induced lung injury. American journal of respiratory cell and molecular biology. 2003; 28(5):600–6. Epub 2003/04/23. https://doi.org/10.1165/rcmb.2002-0059OC PMID: 12707016.

36. Guillot S, Delaval P, Brinchault G, Caulet-Maugendre S, Depince A, Lena H, et al. Increased extracellular matrix metalloproteinase inducer (EMMPRIN) expression in pulmonary fibrosis. Exp Lung Res. 2006; 32(3–4):81–97. Epub 2006/06/07. https://doi.org/10.1080/01902140600710512 PMID: 16754474.

37. Gwinn WM, Damsker JM, Falahati R, Okwumabua I, Kelly-Welch A, Keegan AD, et al. Novel approach to inhibit asthma-mediated lung inflammation using anti-CD147 intervention. J Immunol. 2006; 177(7):4870–9. Epub 2006/09/20. https://doi.org/10.4049/jimmunol.177.7.4870 PMID: 16982929; PubMed Central PMCID: PMC2855298.

38. Cho JY, Fox DA, Horejsi V, Sagawa K, Skubitz KM, Katz DR, et al. The functional interactions between CD98, beta1-integrins, and CD147 in the induction of U937 homotypic aggregation. Blood. 2001; 98(2):374–82. Epub 2001/07/04. https://doi.org/10.1182/blood.v98.2.374 PMID: 11435306.

39. Xu D, Hemler ME. Metabolic activation-related CD147-CD98 complex. Mol Cell Proteomics. 2005; 4(8):1061–71. Epub 2005/05/20. https://doi.org/10.1074/mcp.M400207-MCP200 PMID: 15901826; PubMed Central PMCID: PMC1351277.

40. Crosnier C, Bustamante LY, Bartholdson SJ, Bei AK, Theron M, Uchikawa M, et al. Basigin is a receptor essential for erythrocyte invasion by Plasmodium falciparum. Nature. 2011; 480(7378):534–7. Epub 2011/11/15. https://doi.org/10.1038/nature10606 PMID: 22080952; PubMed Central PMCID: PMCPMC3245779.

41. Pushkarsky T, Zybarth G, Dubrovsky L, Yurchenko V, Tang H, Guo H, et al. CD147 facilitates HIV-1 infection by interacting with virus-associated cyclophilin A. Proc Natl Acad Sci U S A. 2001; 98 (11):6360–5. Epub 2001/05/17. https://doi.org/10.1073/pnas.111583198 PMID: 11353871; PubMed Central PMCID: PMCPMC33473.

42. Joseph J, Knobler RL, Lublin FD, Burns FR. Regulation of the expression of intercellular adhesion molecule-1 (ICAM-1) and the putative adhesion molecule Basigin on murine cerebral endothelial cells by MHV-4 (JHM). Adv Exp Med Biol. 1993; 342:389–91. Epub 1993/01/01. https://doi.org/10.1007/978-1-4615-2996-5_60 PMID: 7911643.

43. Kasinrerk W, Tokrasinwit N, Phunpae P. CD147 monoclonal antibodies induce homotypic cell aggregation of monocytic cell line U937 via LFA-1/ICAM-1 pathway. Immunology. 1999; 96(2):184–92. Epub 1999/05/08. https://doi.org/10.1046/j.1365-2567.1999.00653.x PMID: 10233694; PubMed Central PMCID: PMCPMC2326738.

44. Xu Q, Cao JS, Zhang XM. Liver-infiltrating T lymphocytes cause hepatocyte damage by releasing humoral factors via LFA-1/ICAM-1 interaction in immunological liver injury. Inflamm Res. 2002; 51 (1):44–50. Epub 2002/02/16. PMID: 11845998.

45. Matsumoto G, Tsunematsu S, Tsukinoki K, Ohmi Y, Iwamiya M, Oliveira-dos-Santos A, et al. Essential role of the adhesion receptor LFA-1 for T cell-dependent fulminant hepatitis. J Immunol. 2002; 169 (12):7087–96. Epub 2002/12/10. https://doi.org/10.4049/jimmunol.169.12.7087 PMID: 12471145.

46. Ohteki T, Maki C, Koyasu S, Mak TW, Ohashi PS. Cutting edge: LFA-1 is required for liver NK1.1+TCR alpha beta+ cell development: evidence that liver NK1.1+TCR alpha beta+ cells originate from multiple pathways. J Immunol. 1999; 162(7):3753–6. Epub 1999/04/14. PMID: 10201888.

47. Bataller R, Gabele E, Parsons CJ, Morris T, Yang L, Schoonhoven R, et al. Systemic infusion of angiotensin II exacerbates liver fibrosis in bile duct-ligated rats. Hepatology. 2005; 41(5):1046–55. Epub 2005/04/21. https://doi.org/10.1002/hep.20665 PMID: 15841463.

48. Hamzavi J, Ehnert S, Godoy P, Ciuclan L, Weng H, Mertens PR, et al. Disruption of the Smad7 gene enhances CCI4-dependent liver damage and fibrogenesis in mice. J Cell Mol Med. 2008; 12(5B):2130–44. Epub 2008/02/13. https://doi.org/10.1111/j.1582-4934.2008.00262.x PMID: 18266971; PubMed Central PMCID: PMCPMC4506177.

49. Sato T, Ota T, Watanabe M, Imada K, Nomizu M, Ito A. Identification of an active site of EMMPRIN for the augmentation of matrix metalloproteinase-1 and -3 expression in a co-culture of human uterine cervical carcinoma cells and fibroblasts. Gynecol Oncol. 2009; 114(2):337–42. Epub 2009/05/12. https://doi.org/10.1016/j.ygyno.2009.04.004 PMID: 19427027.

50. Sato T, Watanabe M, Hashimoto K, Ota T, Akimoto N, Imada K, et al. A novel functional site of extracellular matrix metalloproteinase inducer (EMMPRIN) that limits the migration of human uterine cervical carcinoma cells. Int J Oncol. 2012; 40(1):236–42. Epub 2011/10/14. https://doi.org/10.3892/ijo.2011.1224 PMID: 21994090.

51. Huang L-R, Wohlleber D, Reisinger F, Jenne CN, Cheng R-L, Abdullah Z, et al. Intrahepatic myeloid-cell aggregates enable local proliferation of CD8+ T cells and successful immunotherapy against chronic viral liver infection. Nat Immunol. 2013; 14(6):574–83. https://doi.org/10.1038/ni.2573 http://www.nature.com/ni/journal/v14/n6/abs/ni.2573.html#supplementary-information. PMID: 23584070

52. Kassel R CM, Lezzoni JC, Taylor NA, Pruett T, Hahn YS. Chronically Inflamed Livers Up-regulate Expression of Inhibitory B7 Family Members. Hepatology. 2010; 50(5):1625–37.

53. MacDonald HR, Lees RK, Bron C. Cell surface glycoproteins involved in the stimulation of interleukin 1-dependent interleukin 2 production by a subline of EL4 thymoma cells. I. Functional characterization by monoclonal antibodies. J Immunol. 1985; 135(6):3944–50. Epub 1985/12/01. PMID: 2415592.

54. Howard RB, Christensen A.K., Gibbs F.A., Pesch L.A. The enzymatic preparation of isolated intact parenchymal cells from rat liver. J Cell Biol. 1967; 35(3):675–84. https://doi.org/10.1083/jcb.35.3.675 PMID: 4294245

55. Shackel NA, McGuinness PH, Abbott CA, Gorrell MD, McCaughan GW. Insights into the pathobiology of hepatitis C virus-associated cirrhosis: analysis of intrahepatic differential gene expression. Am J Pathol. 2002; 160(2):641–54. Epub 2002/02/13. https://doi.org/10.1016/S0002-9440(10)64884-5 PMID: 11839585; PubMed Central PMCID: PMCPMC1850631.

56. Choi WG, Han J, Kim JH, Kim MJ, Park JW, Song B, et al. eIF2alpha phosphorylation is required to prevent hepatocyte death and liver fibrosis in mice challenged with a high fructose diet. Nutr Metab (Lond). 2017; 14:48. Epub 2017/08/07. https://doi.org/10.1186/s12986-017-0202-6 PMID: 28781602; PubMed Central PMCID: PMCPMC5537942.

57. Nevzorova YA, Bangen JM, Hu W, Haas U, Weiskirchen R, Gassler N, et al. Cyclin E1 controls proliferation of hepatic stellate cells and is essential for liver fibrogenesis in mice. Hepatology. 2012; 56 (3):1140–9. Epub 2012/03/29. https://doi.org/10.1002/hep.25736 PMID: 22454377; PubMed Central PMCID: PMCPMC3396430.

58. Bhathal PS, Rose N.R., Mackay I.R., Whittingham S. Strain differences in mice in carbon tetrachloride-induced liver injury. Br J Exp Pathol. 1983; 64(5):524–33. PMID: 6639871

59. Sancho-Bru P, Bataller R, Gasull X, Colmenero J, Khurdayan V, Gual A, et al. Genomic and functional characterization of stellate cells isolated from human cirrhotic livers. J Hepatol. 2005; 43(2):272–82. https://doi.org/10.1016/j.jhep.2005.02.035 PMID: 15964095.

60. Khunkaewla P, Schiller HB, Paster W, Leksa V, Cermak L, Andera L, et al. LFA-1-mediated leukocyte adhesion regulated by interaction of CD43 with LFA-1 and CD147. Mol Immunol. 2008; 45(6):1703–11. Epub 2007/11/13. https://doi.org/10.1016/j.molimm.2007.09.032 PMID: 17996943.

61. Hao JL, Cozzi PJ, Khatri A, Power CA, Li Y. CD147/EMMPRIN and CD44 are potential therapeutic targets for metastatic prostate cancer. Curr Cancer Drug Targets. 2010; 10(3):287–306. Epub 2010/04/08. https://doi.org/EPub-Abstract-CCDT-34 [pii]. PMID: 20370680.